I.J. Wireless and Microwave Technologies, **2021, 1, 15-21**
Published Online February 2021 in MECS (http://www.mecs-press.org/)
DOI: 10.5815/ijwmt.2021.01.02

Design of a Compact Fractal Unit Cell Absorber for the 2.45 GHz Band

Akaa Agbaeze Eteng
Department of Electrical/Electronic Engineering, Faculty of Engineering, University of Port Harcourt, Port Harcourt, Nigeria.
Email: akaa.eteng@gmail.com

Received: 29 December 2020; Revised: 01 January 2021; Accepted: 12 January 2021; Published: 08 February 2021

Abstract: This paper presents the design of a fractal unit cell absorber for electromagnetic energy absorption in the 2.45 GHz band. The configuration is based on a second-order Minkowski-inspired fractal geometry, through which a compact structure is realized. The proposed design is achieved using full-wave electromagnetic simulations and the study of an equivalent circuit model. At 2.45 GHz, the synthesized structure achieves a near-perfect absorptivity of 99%, with a modest footprint of 0.11λ. The realized structure can serve as a constituent element for the design of absorber arrays to mitigate multipath effects and prevent eavesdropping attacks in indoor wireless environments.

Index Terms: Electromagnetic absorber, metamaterial, Minkowski fractal, unit cell

1. Introduction

Electromagnetic energy absorbers are specially synthesized structures which neither reflect nor transmit incident electromagnetic waves at specified frequencies. These structures find useful application in the mitigation of multipath reflections, such as in anechoic chambers [1]. The suppression of multipath also enables secure communications in indoor wireless environments, by impeding eavesdropping attacks [2]. Metamaterials are good candidates for the implementation of absorbers, due to their unique abilities to modify electromagnetic wave responses, and the small sizes that can be realized with their use [3,4]. Typically, these absorbers are synthesized with their impedance matched to the free-space impedance in order to prevent reflection of incident electromagnetic energy. Surface-oriented implementations usually consist of a repetitive conductive pattern – the unit cell, on a lossy dielectric substrate, backed by a ground plane. However, all-dielectric configurations have also been realized [5–7]. The energy absorption properties of constituent unit cells are critical to the performance of the bulk structure.

Split ring resonators (SRRs) [8], and complementary-SRRs [9,10] are among the more popular planar metamaterial unit cell configurations, and have been employed for realizing planar absorbers [8,11,12]. Fractal geometries are also being studied as plausible unit cell configurations [13–17]. Minkowski fractal geometries, in particular, are attractive for their ability to enable physically smaller conductive patches without compromised electrical lengths [13,14]. In these investigations, first-order iterations of the fractal geometry were employed with the aim of realizing compact designs. In furtherance of this objective, a fractal geometry inspired by the second-order Minkowski fractal is proposed in this paper as a unit cell configuration for electromagnetic energy absorption at 2.45 GHz. The structure offers a compact footprint of 0.11λ, where λ is the free-space wavelength at the operating frequency. Simulations reveal a low reflection coefficient of approximately -20 dB at 2.45 GHz, which translates to an absorption peak of about 99% at this frequency.

The rest of the paper is organized as follows. In section 2, an equivalent circuit model (ECM) of a simple patch unit cell is presented, which is used along with parametric studies to gain necessary insights into the behavior of the unit cell in section 3. These insights are employed to design the fractal unit cell in section 4, while section 5 concludes the paper.

2. Unit cell Absorber Equivalent Circuit Model

An equivalent circuit model (ECM) is a key analytic tool for gaining insights into relationships between the physical structure unit cells, and their electromagnetic behavior. This study proceeds by assuming a simple unit cell structure, composed of a dielectric substrate sandwiched between a top-layer conducting patch and a ground plane on the bottom layer, made of similar conducting material, as illustrated in Fig. 1a. The ECM describing this configuration is a transmission line (TL) model, shown in Fig 1b, which consists of a series RLC-circuit in parallel with a grounded substrate impedance [13,18].

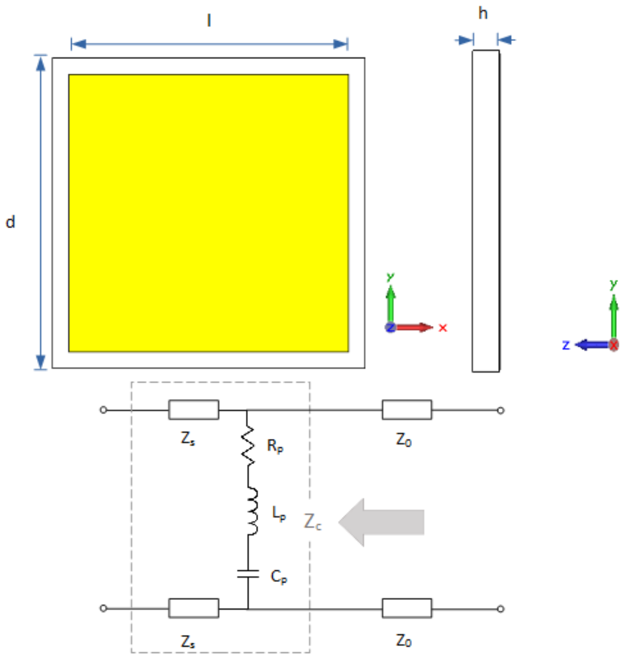

Fig.1. Simple patch unit cell structure with equivalent circuit model

Z_s is the complex impedance of the substrate with a ground plane, and Z_p is the complex impedance of the top-layer conducting patch, given by

$$Z_p = R_p + \frac{1-\omega^2 L_p C_p}{j\omega C_p} , \tag{1}$$

where R_p, L_p and C_p are the patch resistance, inductance and capacitance at the resonant frequency ω.

Similarly, the cell impedance at resonance can be decomposed into a series RLC-circuit, namely

$$Z_c = R_c + \frac{1-\omega^2 L_c C_c}{\omega C_c} , \tag{2}$$

where the subscript c denotes equivalent circuit values for the unit cell at the resonant frequency ω.

For a physical interpretation of the unit cell RLC parameters, R_c represents the resistance of the conducting patch and ground plane layers coupled to the resistance of the lossy dielectric substrate. L_c represents the inductance of the unit cell structure, which consists of the self-inductance of the conducting layers on both sides of the dielectric substrate, and the mutual inductance between them. C_c , on the other hand, consists mainly of the parallel plate capacitance developed as a consequence of having a dielectric material sandwiched between two conducting plates, as well as capacitances resulting from fringing fields at the edges of the structure.

Perfect absorption of incident EM energy at the resonant frequency is achieved when the unit cell impedance is matched to the free-space impedance Z_0. In other words, this requires that at ω, $Z_c = R_c = 377\Omega$. Consequently, the primary objective in the design of a unit cell absorber is to ensure that $R_c = 377\Omega$, and $\mathrm{Im}\{Z_c\} = 0$ at the resonant frequency. This objective can be succinctly characterized as a minimization of the reflection coefficient

$$\Gamma = \frac{\mathrm{Re}\{Z_c\} - Z_0}{\mathrm{Re}\{Z_c\} + Z_0} , \tag{3}$$

where the optimum value of $\Gamma = 0$ is desired.

Consequently, EM energy absorption for the unit cell structure can be defined as

$$A = 1 - |\Gamma|^2 \quad (4)$$

3. Parametric Study of Patch Unit cell Absorber

In order to gain insights into the impact of physical parameters on the absorption performance of a unit cell structure, a simple patch unit cell absorber is designed for operation at 2.45 GHz. The square unit cell has a dimension d $= \lambda/4$, where λ refers to the free-space wavelength at the operating frequency (Fig 1a). The unit cell is modelled using an FR4 substrate (ε_r = 4.4, $\tan\delta$ =0.02) of thickness 1.6 mm. The length of the conducting patch is optimized for resonance at 2.45 GHz (i.e l = 27.36 mm) using CST Microwave Studio (2015). Parameter values for the unit cell equivalent circuit model are extracted using EM simulations and circuit co-simulations in CST Design Studio (2015). Fig 2 shows the impedance, the reflection coefficient and the absorptivity of the 2.45 GHz patch unit cell, while the extracted equivalent circuit values for the unit cell at 2.45 GHz are presented in Table 1.

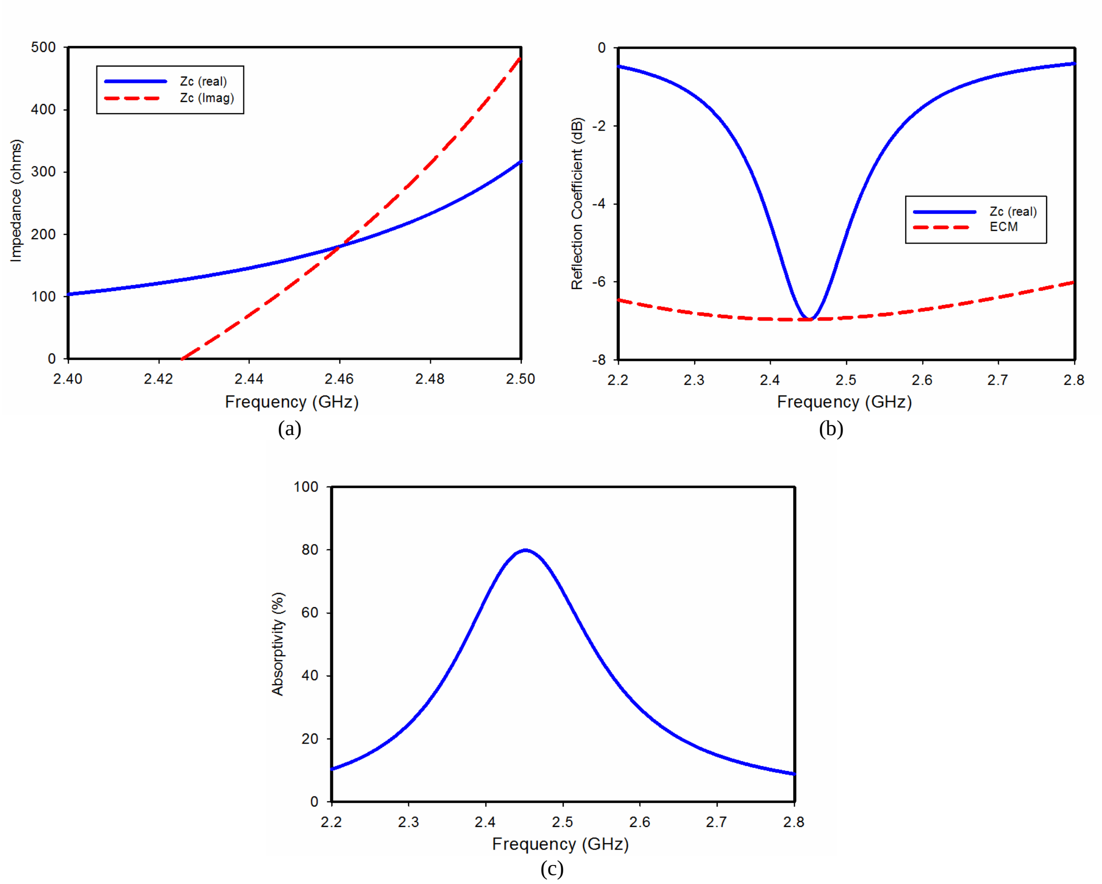

Fig. 2. (a) Impedance, (b) reflection coefficient and the (c) absorptivity of unit cell structure

Table 1. Equivalent circuit model values for square patch unit cell at 2.45 GHz

Parameter	R_c (Ω)	L_c (nH)	C_c (pF)	Im {Z_{cell}} (Ω)
Value	131.20	5.53	0.80	118.08

From the results (Fig 2c) it can be observed that the unit cell achieves 80% absorptivity at 2.45 GHz. This is a consequence of a reflection coefficient of about – 7dB, as shown in Fig 2b. This reflection coefficient value implies that there is some level of mismatch between the impedance of the unit cell and the free-space impedance at the resonant frequency. This is evident from Fig 2a, where at 2.45 GHz, R_c < 377 Ω and $\mathrm{Im}\{Z_c\} \neq$ 0. Furthermore, Fig 2b reveals a good match between the reflection coefficient results obtained using full-wave EM simulations and the equivalent circuit model at 2.45 GHz, which verifies the correctness of the extracted circuit values.

A parametric study is carried out to examine the impact of the unit cell size on its reflection coefficient and absorptivity characteristics. Results of this parametric study are shown in Fig 3, and the corresponding ECM values at 2.45 GHz are listed in Table 2.

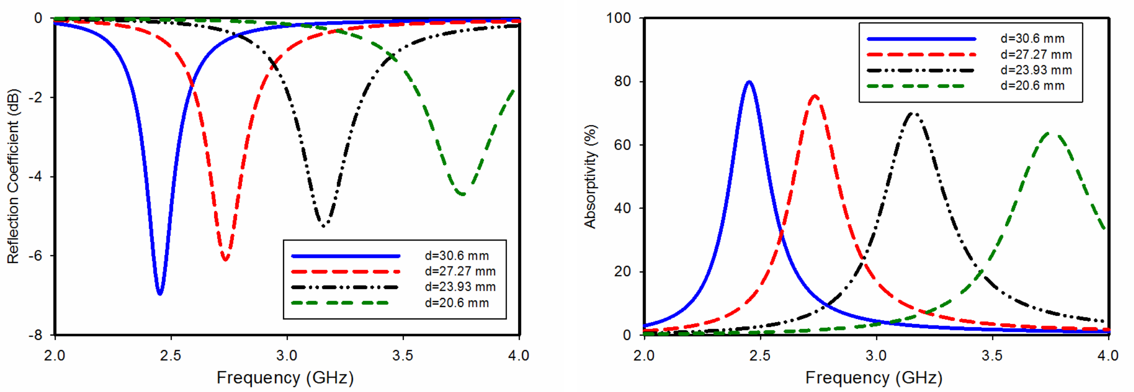

(a) (b)

Fig. 3. Parametric study of impact of unit cell size on (a) reflection coefficient and (b) absorptivity

Table 2. Geometrical and electrical properties of unit cell

Parameter	d=30.6 mm	d=27.27 mm	d=23.93 mm	d=20.6 mm
R_c (Ω)	131.20	144.28	161.31	144.33
L_c (nH)	5.53	0.82	1.89	5.80
C_c (pF)	0.80	1.58	0.68	0.19
f_{res} (GHz)	2.45	2.74	3.16	3.76
Γ (dB)	-6.96	-6.09	-5.25	-4.44

The reflection coefficient plots (Fig 3a) reveal that a reduction in the size of the unit cell leads to an increase in the frequency at which resonance occurs. A reason for this can be adduced from the trends in inductance and capacitance values shown in Table 2. Apart from the first column where the unit cell structure was deliberately optimized for resonance at 2.45 GHz, the capacitance reduces with the size of the unit cell, an observation consistent with electrostatic principles. Also, the Table reveals that the unit cell inductance, which is related to the relative sizes of the conducting patch and ground plane, rises with a reduction in the size of the non-optimal unit cell. The net effect of these trends is that resonance occurs at higher frequencies with smaller unit cell sizes. Furthermore, Fig 3a reveals a progressive rise in the reflection coefficient values at resonant frequencies, which can be attributed to increasing levels of mismatch to the free-space impedance, ultimately leading to a reduction in unit cell absorptivity at the resonant frequencies (Fig 3b).

In the light of the preceding observations, a unit cell miniaturization strategy needs to exert some level of control over the ECM values of the unit cell in order to ensure good absorptivity at 2.45 GHz.

4. Fractal Unit cell Design

In order to miniaturize the unit cell, a fractal patch design based on a second-order Minkowski fractal geometry is adopted. The Minkowski fractal geometry enables longer current paths at the patch edges with reduced patch sizes, compared to a square patch. The evolution of the unit cell patch is illustrated in Fig 4. In the first iteration, squares of dimension $s_1 \times l$ are cut out from the sides of the initial square patch of dimension l. In the second iteration, squares of dimension $s_1^2 \times l$ are removed from the edges realized in the first iteration. By so doing, the effective length of the patch becomes

$$l_{eff} = l\left(1+2s_1+6s_1^2\right) \approx \frac{\lambda}{4}, \tag{5}$$

so that

$$l \approx \frac{\lambda}{4\left(1+2s_1+6s_1^{\,2}\right)}. \tag{6}$$

In order to minimize the dimension l, the factor s_1 is chosen as 0.3 [13]. Consequently, the miniaturization process aims to reduce the size of the unit cell by a factor of approximately 2.14. In order to compensate for low unit cell capacitance value occasioned by the smaller patch size, a thinner dielectric substrate with a higher relative permittivity is chosen, namely Rogers TMM 10i (ε_r = 9.8, $\tan\delta$ =0.002, thickness = 0.508 mm).

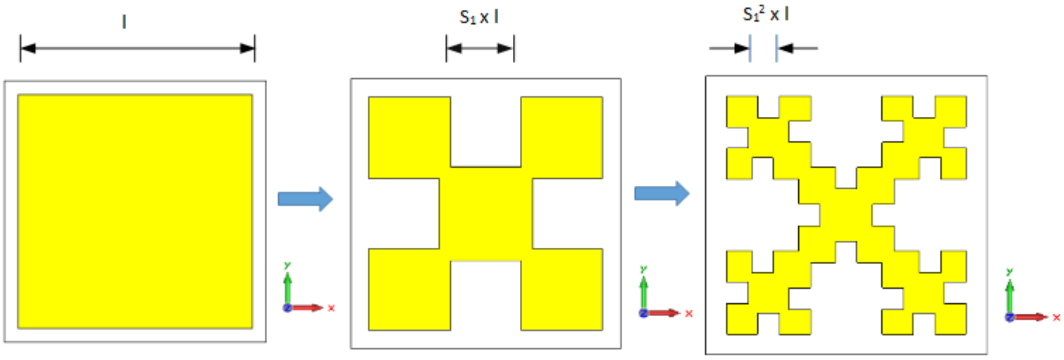

Fig. 4. Iterative design of fractal patch

Table 3 contains the dimensions of the fractal unit cell, which has been optimized in the full-wave solver. The optimized fractal unit cell is realized with an overall size of 13.67 mm, which is approximately 0.11λ at the operating frequency of 2.45 GHz. The extracted ECM values of the fractal unit cell are similarly listed in Table 4, which, in comparison to Table 1, reveal impedance values closer to providing a match to the free-space impedance of 377 **Ω**. The resulting reflection coefficient of approximately – 20dB is shown in Fig 5a, which also demonstrates the accuracy of the extracted model parameters at 2.45 GHz. Fig 5b similarly reveals that the optimized fractal unit cell structure achieves a near-perfect absorptivity of 99% at 2.45 GHz.

Table 3. Fractal patch dimensions

Parameter	d	l	s_1	h
Value (mm)	13.67	12.67	0.3	0.508

Table 4. Equivalent circuit model values of fractal unit cell at 2.45GHz

Parameter	R_c (Ω)	L_c (nH)	C_c (pF)	Im $\{Z_{cell}\}$ (Ω)
Value	313.24	0.85	15.30	-12.85

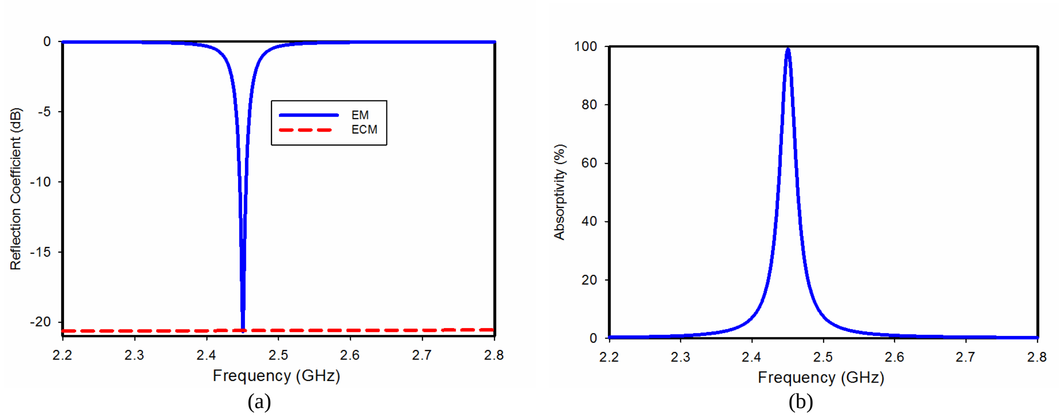

Fig. 5 (a) Reflection coefficient and (b) absorptivity of fractal unit cell

Table 5 compares the designed fractal unit cell absorber with similar absorber designs. It can be seen that the proposed fractal absorber achieves a good degree of miniaturization, while providing comparable absorptivity performance at the operating frequency.

Table 5. Comparison with related works

Reference	Frequency (GHz)	Size	Absorptivity (%)
[17]	2.45	0.12λ	99
[13]	0.868	0.25λ	99
[19]	5	0.30 λ	99
This work	2.45	0.11λ	99

5. Conclusion

This paper has demonstrated the design of a compact unit cell absorber based on a second-order Minkowski-inspired fractal geometry. The proposed unit cell has a footprint of 0.11λ, which offers a good degree of miniaturization compared to similar microwave absorber cell structures. The structure provides a near-perfect absorption peak of 99% at the working frequency of 2.45 GHz. As an extension of this work, further investigations will seek to employ the proposed fractal unit cell in array configurations to realize planar surfaces for microwave energy absorption and harvesting.

References

[1] Ali Z, Muneer B, Shankar Chowdhry B, et al. Design of Microwave Pyramidal Absorber for Semi Anechoic Chamber in 1 GHz~20 GHz range. Int. J. Wirel. Microw. Technol. 2020;10:22–29.
[2] Tsiftsis TA, Valagiannopoulos C, Liu H, et al. Metasurface-Coated Devices: A New Paradigm for Energy-Efficient and Secure Communications in 5G and Beyond. arXiv:2006.12044 [eess] [Internet]. 2020;1–8. Available from: http://arxiv.org/abs/2006.12044.
[3] Landy NI, Sajuyigbe S, Mock JJ, et al. Perfect metamaterial absorber. Phys. Rev. Lett. 2008;100.
[4] Wen Q-Y, Zhang H-W, Yang Q-H, et al. Perfect Metamaterial Absorbers in Microwave and Terahertz Bands. Metamaterial. 2012;
[5] Liu X, Fan K, Shadrivov I V., et al. Experimental realization of a terahertz all-dielectric metasurface absorber. Opt. Express. 2017;25:191.
[6] Luo H, Cheng Y. Dual-band terahertz perfect metasurface absorber based on bi-layered all-dielectric resonator structure. Opt. Mater. (Amst). [Internet]. 2019;96:109279. Available from: https://doi.org/10.1016/j.optmat.2019.109279.
[7] Luo H, Cheng Y. Thermally tunable terahertz metasurface absorber based on all dielectric indium antimonide resonator structure. Opt. Mater. (Amst). [Internet]. 2020;102:109801. Available from: https://doi.org/10.1016/j.optmat.2020.109801.
[8] Yudistira HT, Ginting LY, Kananda K. High absorbance performance of symmetrical split ring resonator (SRR) terahertz metamaterial based on paper as spacer. Mater. Res. Express [Internet]. 2018;6:025804. Available from: https://iopscience.iop.org/article/10.1088/2053-1591/aaf27e.
[9] Kaur J. Dual Band High Directivity Microstrip Patch Antenna RotatedStepped-Impedance Array Loaded with CSRRs for WLAN Applications. Int. J. Wirel. Microw. Technol. 2016;6:1–11.
[10] A. Saleh A, S. Abdullah A. A Novel Design of Patch Antenna Loaded with Complementary Split-Ring Resonator and L- Shape Slot for (WiMAX/WLAN) Applications. Int. J. Wirel. Microw. Technol. 2014;4:16–25.
[11] Zhao J, Cheng Y. Ultrabroadband Microwave Metamaterial Absorber Based on Electric SRR Loaded with Lumped Resistors. J. Electron. Mater. 2016;45:5033–5039.
[12] Moghbeli E, Askari HR, Forouzeshfard MR. The effect of geometric parameters of a single-gap SRR metamaterial on its electromagnetic properties as a unit cell of interior invisibility cloak in the microwave regime. Opt. Laser Technol. [Internet]. 2018;108:626–633. Available from: https://doi.org/10.1016/j.optlastec.2018.07.025.
[13] Venneri F, Costanzo S, Di Massa G. Fractal-Shaped Metamaterial Absorbers for Multireflections Mitigation in the UHF Band. IEEE Antennas Wirel. Propag. Lett. 2018;17:255–258.
[14] Venneri F, Costanzo S. Fractal microwave absorbers for multipath reduction in UHF-RFID systems. Adv. Intell. Syst. Comput. 2017;570:1008–1013.
[15] Venneri F, Costanzo S, Borgia A. A dual-band compact metamaterial absorber with fractal geometry. Electron. 2019;8:2–9.
[16] Ma YB, Zhang HW, Li YX. Study on a novel dual-band metamaterial absorber by using fractal Koch curves. Wuli Xuebao/Acta Phys. Sin. 2014;63:1–7.
[17] Costanzo S, Venneri F. Innovative Fractal-Based Metasurface for Energy Harvesting. URSI GASS [Internet]. Rome; 2020. p. 1–3. Available from: http://www.ursi.org/proceedings/procGA20/papers/PID6351651.pdf.
[18] Costa F, Genovesi S, Monorchio A, et al. A circuit-based model for the interpretation of perfect metamaterial absorbers. IEEE Trans. Antennas Propag. 2013;61:1201–1209.

[19] Amiri M, Tofigh F, Shariati N, et al. Wide-angle metamaterial absorber with highly insensitive absorption for TE and TM modes. Sci. Rep. [Internet]. 2020;10:1–13. Available from: https://doi.org/10.1038/s41598-020-70519-8.

Author’s Profile

Akaa Agbaeze Eteng obtained a B.Eng degree in Electrical/Electronic Engineering from the Federal University of Technology Owerri, Nigeria in 2002, and a M. Eng. degree in Telecommunications and Electronics from the University of Port Harcourt, Nigeria in 2008. In 2016, he obtained a Ph.D. in Electrical Engineering from Universiti Teknologi Malaysia. He is currently a lecturer at the Department of Electrical/Electronic Engineering at the University of Port Harcourt, Nigeria. His research interests include wireless energy transfer, radio frequency energy harvesting, and wireless powered communications.

How to cite this paper: Akaa Agbaeze Eteng, " Design of a Compact Fractal Unit Cell Absorber for the 2.45 GHz Band", International Journal of Wireless and Microwave Technologies(IJWMT), Vol.11, No.1, pp. 15-21, 2021.DOI: 10.5815/ijwmt.2021.01.02